

Published in final edited form as:

Neuroimage. 2009 August ; 47(Suppl 2): T143–T151. doi:10.1016/j.neuroimage.2008.10.067.

Computerized assessment of vessel morphological changes during treatment of glioblastoma multiforme: Report of a case imaged serially by MRA over four years

Elizabeth Bullitt¹, Matthew Ewend¹, James Vredenburg², Allan Friedman², Weili Lin¹, Kathy Wilber¹, Donglin Zeng¹, Stephen R. Aylward³, and David Reardon²

¹ CASILab, CB # 7062, University of North Carolina, Chapel Hill, NC 27599, USA

<http://casilab.med.unc.edu/>{ bullitt@med.unc.edu, ewend@med.unc.edu, weili_lin@med.unc.edu, kwilber@med.unc.edu}; dzeng@bios.unc.edu

² The Preston Robert Tisch Brain Tumor Center at Duke, DUMC Box 3624, Durham, NC 27710, USA james.vredenburg@duke.edu; { fried010@mc.duke.edu, reard003@mc.duke.edu}

³ Kitware, 28 Corporate Drive, Clifton Park, NY, 12065 Stephen.Aylward@Kitware.com

Abstract

A patient with glioblastoma multiforme underwent serial computerized analysis of tumor-associated vasculature defined from magnetic resonance angiographic (MRA) scans obtained over almost a four year period. The clinical course included tumor resection with subsequent radiation therapy, a long symptom-free interval, emergence of a new malignant focus, resection of that focus, a stroke, and treatment with chemotherapy and anti-angiogenic therapy. Image analysis methods included segmentation of vessels from each MRA and statistical comparison of vessel morphology over 4 regions of interest (the initial tumor site, the second tumor site, a distant control region, and the entire brain) to the same 4 regions of interest in 50 healthy volunteers (26 females and 24 males; mean age 39 years). Results suggested that following completion of focal radiation therapy (RT) vessel shape abnormalities, if elevated at the time of RT completion, may progressively normalize for months in focal regions, that progressively severe vessel shape abnormalities can precede the emergence of a gadolinium enhancing lesion by months, that lesion resection can produce a dramatic but highly transient drop in abnormal vessel tortuosity both focally and globally, and that treatment with anti-angiogenic agents does not necessarily normalize vessel shape. Quantitative measurements of vessel morphology as defined from MRA may provide useful insights into tumor development and response to therapy.

Keywords

MRA; tumor; vessel; computer; tortuosity; glioblastoma; brain

Communicating author: Elizabeth Bullitt, MD, CASILab, CB # 7062, University of North Carolina, Chapel Hill, NC 27599, USA, Telephone (919) 843-3101 or (919) 489-3125, Fax (919) 843-1500, bullitt@med.unc.edu.

Potential Conflicts of Interest

Software for generic vessel segmentation has been licensed to Medtronic Corp (Minn., Minn), R2 Technologies (Alta Vista CA), Kitware (Rochester NY), and WL Gore and Associates (Flagstaff, AZ). The software has additionally been licensed for research use to multiple universities. No licensed group has been involved with the currently described work either directly or indirectly.

Publisher's Disclaimer: This is a PDF file of an unedited manuscript that has been accepted for publication. As a service to our customers we are providing this early version of the manuscript. The manuscript will undergo copyediting, typesetting, and review of the resulting proof before it is published in its final citable form. Please note that during the production process errors may be discovered which could affect the content, and all legal disclaimers that apply to the journal pertain.

1. Introduction

Glioblastoma multiforme is the most common adult brain malignancy (CBTRUS-2006). The prognosis has generally been regarded as bleak, with median survival of about 12 months from the time of diagnosis (Wong and Brem 2007; Krex et. al., 2007). Recent advances in the understanding of tumor biology, however, have led to new therapeutic agents that can prolong the lives of these patients, sometimes for years (Iwadate et. al., 2003; Floeth et. al., 2003; Stupp et. al., 2003; Reardon et. al., 2006; Vredenburgh et. al., 2007; Wong and Brem 2007; Parvez 2008, Sampson et. al., 2008).

Given the ongoing development of new therapeutic agents, there is genuine need of a method that can effectively monitor treatment efficacy. The current standard of practice is to estimate tumor volumes from sequential sets of gadolinium-enhanced, T1 images (Therese et. al., 2000; Warren et. al., 2001; Dempsey et. al., 2005). Other groups have applied similar methods to T2 images, under the reasonable assumption that the “edema” visible on T2 images consists of a combination of edema and tumor infiltration (Shukla 2005). Such assessments depend upon comparison of current to past volumes, do not directly evaluate what the tumor will do next, and are readily confounded by the necrosis that may appear with successful radiation therapy or chemotherapy, since such necrosis can induce enhancement and edema indistinguishable from that of tumor growth. Moreover, glioblastomas are deeply infiltrative, and tumor cells may extend well beyond gadolinium enhancing margins or even the margins of tumor-associated edema (Burger 1991). Diffusion tensor imaging is a magnetic resonance (MR) imaging method that shows promise in tumor assessment (Price 2006), but like T1 and T2 imaging assesses only structural changes.

A reliable method of assessing tumor metabolic or physiologic activity noninvasively would be of value. MR spectroscopy and Positron Emission Tomography (PET) are two imaging methods under investigation by several groups. An alternative approach is to evaluate tumor vasculature. Tumor growth beyond minimal size is dependent upon angiogenesis, the process of new blood vessel formation from existing vessels (Folkman 1971). Vessels are recruited via the expression of agents such as Vascular Endothelial Growth Factor (VEGF) and other growth factors (Ferrara et. al., 1996, McDonald and Baluk 2002). These factors alter the vessel wall, producing both structural and permeability changes (McDonald and Baluk 2002, Saaristo et. al., 2002, Yoo et. al., 2005). Cancer-associated changes to vascular morphology occur very early during tumor growth. Indeed, within 24 hours of injection of only a few cancer cells, initially healthy vessels in the tumor vicinity develop tortuosity abnormalities with such changes emerging prior to angiogenic sprouting (Li et. al., 2000). These changes affect vessels lying well outside of the tumor margins (Li et. al., 2000). These vessel tortuosity abnormalities appear across cancer types, and have been aptly described by Baish as “many smaller bends upon each larger bend” (Baish and Jain 2000). With time, abnormal vessel tortuosity can sometimes spread to even major named vessels, with MR-apparent alterations occurring a centimeter or more outside of any T1-gadolinium enhancing lesion (Bullitt et. al., 2007).

The majority of the literature addressing *in vivo* imaging of tumor-associated vasculature has concentrated upon the “microvasculature” as perceived by perfusion and permeability imaging. An alternative approach is to quantitatively assess “macrovascular” vessel morphology as perceived by magnetic resonance angiography (MRA). This approach cannot assess vessels of diameter smaller than that of the voxel size used during image acquisition, thus precluding evaluation of tiny neoangiogenic sprouts, nor can it assess vessel permeability. It does, however, permit quantitative, statistical assessment of parameters such as vessel number, vessel radius, and vessel tortuosity. In one blinded study, quantitative, MRA-based measures of vessel tortuosity were able to correctly define all but one of 30 brain tumors as benign or

malignant when imaged prior to total gross resection (Bullitt et. al., 2005). Another study addressed the treatment of brain metastases from breast cancer and found that measurements of vessel tortuosity appeared to predict the likelihood of treatment failure one to two months prior to analysis of tumor size (Bullitt et. al., 2007). In a different study of genetically engineered mice, vessel tortuosity assessments were capable of correctly detecting emerging malignancy for carcinomas larger than 1mm³ (Bullitt et. al., 2006). Additionally, vessel shape abnormalities appear to resolve with successful treatment (Yuan et. al., 1996; Li et. al., 2000, Jain 2001, Bullitt et. al., 2007).

Almost all prior studies assessing tumor vasculature in human patients have been either cross-sectional studies, in which large numbers of patients are imaged at a single time, or brief longitudinal studies in which each patient is imaged at a few times during a particular form of treatment. This paper describes sequential MRA imaging of a single glioblastoma patient over a period of almost four years. This patient's course was complex and illustrates many of the problems inherent to assessing tumor activity in the actual clinical arena. This case also illustrates several points relevant to the timing and location of vessel morphological changes during tumor treatment. Throughout this paper, we use the term "lesion" to define tumor margins on gadolinium-enhanced T1 images, "edema" to indicate associated hypo/hyperintensity on T1/T2 images (regardless of whether this finding is due to edema, tumor infiltration, or both), and "region" to describe the combination of lesion and edema.

2. Clinical History

A 55-year old Caucasian male developed intermittent dyslexia. Evaluation revealed a 5.5 cm³, ring-enhancing left temporal lobe lesion with a small amount of associated edema (Fig. 1A). On 8/7/03 (month 0 of the patient's clinical course) he underwent a gross total resection with insertion of carmustine wafers (GLIADEL[®] Wafer, MGI Pharma, USA) into the resection cavity (Fig 1B). Pathology confirmed the diagnosis of glioblastoma (GBM; World Health Organization glioma grade IV). Postoperatively he had no neurologic deficit.

The patient underwent conventional external, fractionated beam radiotherapy (6120 cGy to the tumor bed and an additional 4500 cGy that included the surrounding edematous region) with concurrent temozolomide (200mg/m² on days 1–5 every 28 days), followed by two cycles of lomustine (110 mg/m²) complicated by neutropenia necessitating dose reduction of the second cycle (82.5 mg/m²). He then (month 5) elected to discontinue chemotherapy. He remained active, neurologically intact, and continued to work as a teacher. Routine T1 and T2 brain images were acquired every 3–4 months with no evidence of gadolinium enhancement, mass effect, edema, or other sign of tumor.

Thirty-two months after the original diagnosis a new 1.0×1.2×1.5 cm enhancing nodule with associated edema was detected by MR. This lesion was separated by about a centimeter from the initial resection site, and it was initially unclear whether this new lesion represented tumor recurrence or radiation necrosis (Fig 1C). An FDG-PET scan of the brain did not reveal evidence of increased metabolic activity. However, a follow-up brain MRI two months later (month 34) revealed both enlargement of the gadolinium enhancing lesion to 4.5 cm³ and increased edema consistent with recurrent tumor (Fig 1D). A stereotactic biopsy was obtained followed by total gross resection of the new lesion in month 35. Histopathology confirmed the diagnosis of GBM. Immunohistochemical analysis of the tumor sample revealed methylguanine methyltransferase expression in 20% of tumor cells, 80% of tumor cells stained for EGFR, 50% for PTEN, 30% for phosphor-S6 protein, 10% for EGFRvIII and 5% for phosphor-AKT. Postoperatively the patient refused further chemotherapy and initiated a naturopathic regimen. Apart from dyslexia he remained asymptomatic.

A scan during month 37 (Fig 1E), however, suggested an emerging occipital lobe infarction with associated enhancement, some of which may have been tumor or surgically related. The patient was begun on irinotecan 125 mg/m² and bevacizumab 10 mg/kg during month 38, with later downward adjustment in dosage because of neutropenia. Apart from his dyslexia he remained asymptomatic until month 48, at which time he began experiencing new difficulty with word finding (Fig 1F). His therapy was changed to bevacizumab and etoposide, which he continued for another 4 months. The patient and his family then made the decision to discontinue therapy. He died February 2008, 4.5 years from the time of initial diagnosis.

3. Methods

3.1 Image acquisition

This HIPAA-compliant and Institutional Review Board approved study involved quantitative analysis of serial MRA images of the patient described above. As a part of our image processing algorithm, all values calculated from the patient's MRA scans were normalized (z-scored) by values derived from the images of 50 healthy volunteers (aged 19–72 years, mean age 39 years, 26 female 24 male). Our healthy image database is publicly available (<http://insight-journal.org/midas/handle.php?handle=1926/594>) and is not discussed further here. For the patient described in this report, a total of 14 MRA scans were acquired between November 2003, at which time the patient was three months from the time of initial diagnosis and had recently completed radiation therapy, and August 2007, at which time the patient was 48 months from the time of initial diagnosis and had begun to decline neurologically. MRA images were not available prior to month 3 or after month 48 of his clinical course.

MRA scans were all obtained on the same 3T, head only unit (Allegra, Siemens Medical Systems Inc.) using a head coil. Images were acquired using a 3D-time-of-flight sequence without gadolinium injection and that covered the entire head using multiple (5) overlapping (25%) thin slabs (MOTSA). The sequence also employed a magnetization transfer pulse for background suppression of brain parenchyma. The resulting voxel size was $0.5 \times 0.5 \times 0.8$ mm³. The sequence's TR/TE/flip_angle/was 35msec/3msec/22°. Although the base matrix was 448×448, a rectangular FOV of 0.786 and a partial Fourier of 0.8 were employed to reduce data acquisition time to 18 minutes.

Additional, serial, T1-gadolinium enhanced and T2 images were acquired for clinical purposes on either a 3T Siemens Allegra unit (TR/TE=15msec/7msec for T1 and 7730/80 for T2) or a 1.5T Siemens Symphony or Avanto scanner (TR/TE=2100msec/2.5msec for T1 and 2500/80 for T2). Each MRI performed for clinical purposes included multiple additional image sequences that are not discussed further. With the exception of the first MRA sequence, images requested for clinical purposes were performed on a schedule independent of the MRA acquisition schedule and were blinded to the operator analyzing the MRA images until after the MRA analysis was performed.

Image processing—Following image acquisition, the patient's MRA image was transferred to a computer for postprocessing. Image processing time was approximately 1.5 hours. The approach involved a computerized, statistical comparison of measures of vessel shape between the 50 healthy volunteers and those of the patient over 4 patient-specific anatomical regions.

Our methods of vessel shape analysis have been previously described (Bullitt et. al., 2005, 2006, 2007) and are summarized only briefly here. Vessel segmentation was performed from MRA using a Hessian-based method that, proceeding from a seed point, defined an image intensity ridge representing the vessel skeleton and then defined a radius at each point (Aylward and Bullitt 2002). All images were registered affinely via normalized mutual information (Rueckert 2002; Schnabel et. al., 2001) into the coordinate system of the McConnell T1 atlas

(ICBM) so that a region of interest could be mapped into each MRA of the tumor patient as well as into the MRA of each healthy subject. Regions of interest were delineated using a program that defined tumors via polygon drawing and filling on orthogonal cuts through an image volume.

Four patient-specific regions of interest were employed during the current study. The first was the region of tumor and edema as seen on the patient's initial T1-gadolinium enhanced scan (Region 1). Region 1 was mapped into all of the patient's subsequent MRAs. The second was the region of tumor and edema associated with the patient's second lesion as seen just prior to his second operation (Region 2). This second region was mapped to all of the patient's subsequent MRAs and was also retrospectively mapped to all of the patient's previously acquired MRAs. There was overlap between the edematous regions contained in Regions 1 and 2 as well as between the edema associated with lesion 2 and the initial margins of lesion 1. Regions 1 and 2 therefore almost certainly contained vessels in common. The third region was intended as a control region, located as far away as possible from the two tumor sites. We selected the right frontal area and defined a roughly spherical volume of about 20 cm³ for this control region. The fourth region was the entire brain. The same four regions were mapped to all of the patient's 14 MRA scans as well as to the brains of the 50 healthy volunteers.

Vessels were clipped to the region of interest and analysis was performed only upon the vessels or vessel segments contained within each region of interest. Each measured parameter was normalized (z-scored) by the means and standard deviations of the healthy values calculated over the same region of interest. A minimum of 4 vessels was required for analysis. Calculated vessel attributes included:

- a. Normalized vessel count (nVC): The vessel count provides the number of individual, unbranched vessels contained within or passing through the region of interest and provides a measure of vessel density. When normalized (z-scored), a value of -1 indicates a count one standard deviation below the healthy mean and a value of 2.5 a count 2.5 standard deviations above the healthy mean.
- b. Normalized average radius: (nAVRAD) The average radius provides the average radius of all vessel segments clipped to the region of interest.
- c. Normalized Sum of Angles Metric (nSOAM): SOAM is a tortuosity measure that is elevated in the presence of high-frequency, low-amplitude vessel sine waves or coils. SOAM sums the angles between consecutive trios of points along a space curve and normalizes by the path length (Bullitt et. al., 2003). The SOAM for a region of interest is expressed as the average SOAM of the vessels lying within that region. The SOAM value is almost invariably elevated for cancer-associated vasculature.
- d. Normalized Inflection Count Metric (nICM): The ICM is a tortuosity measure that measures larger amplitude curves than SOAM. The ICM counts "inflection points" along each space curve and multiplies this number (plus one) times the total path length and then divides by the distance between endpoints (Bullitt et. al., 2003). The ICM for a region of interest is expressed as the average ICM of the vessels lying within that region. The ICM value is often elevated in the presence of cancer.
- e. Malignancy Probability (MP): The MP provides an estimate of the probability of malignancy on a scale of 0% to 100% and is calculated by an equation that employs nSOAM and nICM (SOAM and ICM normalized by z-scoring against healthy values). The equation was derived from an earlier study of human patients with a variety of tumor types, both benign and malignant, and employed discriminant analysis of multiple vessel shape parameters with the goal of separating benign from malignant tumors (Bullitt et. al., 2005). The term "Malignancy Probability" is not entirely

accurate when applied to the treatment of tumors such as glioblastoma, because glioblastomas will remain potentially malignant even when in remission. The MP in such cases should instead be viewed as providing a measure of tumor activity. During successful treatment, initially high MP values decrease. When a tumor develops and actively grows, initially low MP values increase. When individual tumors are followed over time, an increase or decrease of 20 over the baseline MP is viewed as significant (Bullitt et. al., 2007).

4. Results

Figure 2 illustrates a 3D visualization of segmented vessels as well as the segmented Region 2. To aid the visualization, the vessels have been connected into vessel trees and color coded according to circulatory group. Arrows point to two abnormally tortuous vessels located close to but outside of the tumor boundary as defined from the T1 image.

Tables 1–4 provide results for all calculated vessel parameters for the four regions of interest. Our “Malignancy Probability” (MP) calculation provides a summary measure that weights and combines the two tortuosity values to provide an overall measure of tumor activity. Figures 3–6 provide graphs of MP over time for all four regions of interest.

As shown by Tables 1–4, there was no clear pattern to normalized vessel number in any of the four regions, except that the vessel count tended to be slightly lower than average in the right frontal control region. Average vessel radius tended to be lower than healthy values in the irradiated regions (as assessed by the regions of interest defined by Regions 1 and 2) but with a marked increase in radius immediately following resection of a new active focus. When the entire brain was examined, average radius was greater by more than one standard deviation than the average vessel radius of healthy controls for all but the three earliest time points imaged. This same finding was true for the right frontal control region.

Figures 3–6 provide a graphical summary of the two tortuosity measures over each of the 4 regions. Each of these figures contains colored arrows indicating four important time points: the completion of radiation therapy, the discovery of lesion 2, resection of that lesion, and initiation of bevacizumab therapy. We first discuss events during the first 3 years for each of the 4 regions and then discuss the events of the final year.

Figure 3 illustrates findings over time for Region 1. As shown by Figure 3, initially high vessel shape abnormalities gradually decreased over a period of about a year following completion of radiation therapy. By month 31 the MP in this initial region showed an ominous rise, however, occurring at least a month before a new gadolinium enhancing lesion about a centimeter away was first noted by MR (at which time a PET scan failed to provide evidence of malignancy). It is important to note that from month 3 to month 32 no gadolinium enhancement, no mass effect, and no edema were apparent on any T1 or T2 image.

Figure 4 illustrates findings over time for Region 2, whose defined volume partially overlapped that of Region 1. Similar to the findings for Region 1, MP values were initially high but then dropped by 6 months following completion of radiation therapy (month 9). Increase in vessel shape abnormalities occurred more quickly than in Region 1, however, appearing by month 17 and thus more than a year before new gadolinium enhancement or the presence of edema became apparent by T1 or T2 imaging.

Figure 5 provides summary tortuosity results for the control right frontal region, located far away from the two identified tumor foci. This right frontal region was not implicated as potentially involved by tumor in any T1 or T2 image or by any other intermittently acquired image of any other type. As shown by Figure 5, the results are somewhat noisy but are clearly

different from those represented by Regions 1 and 2. Initial MP values were low. Indeed, MP values averaged low levels of 6%–7% throughout the patient's course and without any clear trend in rise or fall regardless of therapeutic manipulation.

Figure 6 provides MP values for the entire brain. Analysis of the entire brain is of interest since, in the absence of a gadolinium enhancing lesion that can be used to define a particular region of interest, the entire brain may be the only region of interest that is available over which to assess values. Interestingly, the pattern for the entire brain differed from both that of the two tumor regions and for the control region. Initial MP values for the entire brain were low (15%) but exhibited a relatively steady rise up to high levels (90%+) until the time of surgical resection of the new active focus at month 35. Following total gross resection of lesion 2 at month 35, both Regions 1 and 2 as well as the entire brain exhibited an abrupt drop in MP. This improvement was short-lived, however, with gradual return of vessel shape abnormalities to their original high levels within three months. No effect of tumor growth or surgery was observed within the far distant, control, right frontal region.

Evaluation of the effects of the administration of bevacizumab was complicated by the evolution of an occipital lobe stroke, whose location primarily affected the site of Region 2. Two time points could not be analyzed for Region 2 (Figure 4) because only 2 vessels were defined within the region of interest at these time points. For Region 2, subsequent analyses indicated that the degree of vessel shape abnormality appeared to drop significantly from the previous high level (Figure 4). Some of this effect could have been related to bevacizumab therapy and some to the effect of stroke which could have eliminated a part of the tumor focus and its associated vessels. For Region 1, located about a centimeter away, and for the entire brain, the composite effects of occipital lobe stroke and bevacizumab therapy appeared to provide a modest improvement in vessel shape abnormality, with MP values dropping by about 20 points. Although this difference meets our criteria for a significant drop from the initially high value, suggesting at least a partial response to treatment, the MP values continued to remain relatively high in both regions (77–82). The right frontal control region remained unaffected (Fig 5).

5. Discussion

This paper analyzes changes in vessel morphology as perceived by serial MRA scans in a patient with glioblastoma multiforme imaged over a four year period. His course included delivery of radiation therapy and routine chemotherapy, a long symptom-free interval, emergence of a new malignant focus, resection of that focus, evolution of a stroke that almost certainly involved portions of active tumor, and treatment with anti-angiogenic therapy combined with chemotherapy. The complexity of this case provides a good illustration of the difficulty that must be confronted by any method that aims to assess tumor treatment response.

5.1 Comments on the findings of this report

At least four vessel morphological findings should be discussed, including a) response to radiation therapy, b) timing of vessel shape abnormality development during emergence of a new tumor focus, c) response to surgical resection of an identified active focus, and d) response to anti-angiogenic therapy. As is consistent with our earlier studies (Bullitt et. al., 2005,2006, 2007) vessel count and vessel radius were not particularly helpful parameters when defining tumor activity. Our methods cannot delineate vessels smaller than those definable by the voxel size used during MRA acquisition, and so cannot analyze tiny, neoangiogenic, capillary sprouts. Vessel tortuosity measures, however, extend to much larger feeding vessels visualizable by MRA and appear to provide useful information.

a) Response to radiation therapy—Radiation therapy is not a specifically anti-angiogenic treatment, but instead targets all dividing cells. Almost all reports on vessel normalization during treatment have addressed only the administration of fully or partially anti-angiogenic agents when sequential images are acquired over time (Li et. al., 2000; Willett et. al., 2004; Wieldiers et. al., 2006; Bullitt et. al., 2007). Although we do not have data in our own patient prior to initiation of radiotherapy, vessel shapes were highly abnormal in both Regions 1 and 2 immediately following completion of radiation therapy. The first data points in the current report describe vessel shape normalization, as perceived by MRA, following focal radiation therapy and generic (not specifically anti-angiogenic) chemotherapy. For both of the focal regions of interest, one lying fully within the radiation field and the other partially outside it, vessel shape normalization occurred slowly following administration of radiation therapy with these improvements in vessel shape abnormalities requiring many months.

It makes sense that an effective therapy that is not specifically anti-angiogenic should alter vessel shape parameters, however. If the tumor is attacked directly, thus impeding its ability to produce growth factors, there is likely to be a secondary effect upon the neighboring blood vessels. The slow time course of improvement following radiation therapy is also of note, and is in disagreement with previous reports describing more rapid vessel normalization following more specifically anti-angiogenic therapy (Yuan et. al., 1996; Li et. al., 2000; Jain 2001; Willett et. al., 2004; Wieldiers et. al., 2006; Bullitt et. al., 2007). More research is required to assess the relative effects of specifically anti-angiogenic therapy as compared to more generic therapy in terms of both the timing of vessel normalization and the ultimate effect upon clinical outcome. However, this report suggests that vessel morphology can be altered by effective therapeutic measures that are not specifically anti-angiogenic.

b) Timing of vessel shape abnormality development during emergence of a new focus—In this patient, a new focus of enhancement developed 2.5 years following completion of radiation therapy and after a long remission period in which no gadolinium enhancement and no edema was detectable on any T1 or T2 images. PET scan initially did not suggest malignancy, and there was thus a 2–3 month delay before the new lesion was correctly recognized as malignant. The distinction between radiation necrosis and recurrent tumor can be difficult to make, and this problem is common during the treatment of glioblastoma.

Vessel shape abnormalities appeared many months before the onset of gadolinium enhancement in this patient, however. In the specific region in which gadolinium enhancement later appeared, a marked rise in vessel shape abnormality occurred 15 months prior to the development of an enhancing lesion. At the site of the primary lesion, which was separated by about a centimeter from the new emerging focus (but with some voxels and vessels held in common by the defined Regions 1 and 2), vessel shape abnormalities increased significantly at least a month prior to the recognition of gadolinium enhancement and the development of edema by MR. These findings suggest that vessel shape abnormalities appear very early during malignant tumor development. Indeed, other groups have reported that abnormal vessel tortuosity development in initially healthy vessels is one of the earliest steps during emergence of an incipient malignancy (Li et. al., 2000, Folkman 2000). In our own patient, there was no increase in vessel shape abnormality in the far distant right frontal location, used as a control region.

Interestingly, when the entire brain was examined there was no drop in vessel shape abnormality as a result of focal radiation therapy; instead the MP showed a relatively steady rise from the time of the patient's initial scan to the time of surgical resection. We interpret this finding to indicate that there were additional regions outside of our two defined, tumor-associated, focal regions of interest in which vessel abnormalities were present and becoming worse. Our Regions 1 and 2 were defined by the margins of tumor and edema as seen by T1-

gadolinium enhanced MR. Glioblastomas deeply infiltrate tissue, however, and malignant cells can be found even outside of an enhancing lesion and its associated edema as seen by MR (Burger et. al., 1991). The actual tumor margins therefore cannot be accurately defined from traditional MR. Moreover, Li et. al. (2000) have shown that vessel shape abnormalities can spread for long distances beyond the tumor confines even when the tumor margins are known with certainty. Our own group examined concentric rings around the enhancing rims of glioblastomas as seen by MR, concluding that how far vessel shape abnormalities spread in the adjacent tissue is variable, but can be more than 3 cm in some patients (Bullitt et. al., 2004). An example of abnormal vessels lying well outside of tumor confines is shown in Figure 2 for the current patient. We hypothesize that these distant vascular effects result from growth (or other) tumor-induced factors that diffuse through tissue to affect blood vessels that may be located centimeters away from the tumor margins.

The difference in findings in the four regions examined (Regions 1 and 2, control frontal region, and entire brain) underscore, however, that the analysis of different anatomical regions will produce different results, as will also true for any other method of assessing tumor activity. Whereas one portion of the brain may be responding slowly to radiation therapy with death of tumor cells and normalization of the vasculature, other portions of the brain may be experiencing tumor growth. At present, we can only define a focal region of interest once a tumor has reached sufficient size to be apparent by MR. It would be valuable to develop a search program that could detect focal regions of vessel shape abnormality and to flag such regions as requiring careful future follow-up. We are presently attempting to develop such a program.

c) Response to surgical resection—One of the most striking findings in this study was the dramatic and abrupt drop in vessel shape abnormality that occurred following total gross resection of a focal lesion. This drop affected not only Regions 1 and 2 but the entire brain as well. Improvement was very short-lived, however, with a gradual climb to the initial highly abnormal values in all three regions within three months. We believe that the transient drop in the whole brain tortuosity abnormalities can be explained by a combination of two factors: the direct loss through surgical excision of some of the most abnormal vessels in the brain, and the loss of a major focus producing angiogenic agents that spread through tissue to alter vessel morphology at more distant sites. Surgical excision had no effect on the control right frontal region, located far away from the known site of active tumor.

d) Response to anti-angiogenic therapy—Evaluation of the effects of anti-angiogenic therapy were complicated by the fact that the patient experienced a concomitant, evolving occipital lobe stroke that primarily affected Region 2. Evaluation was impossible at two time points for Region 2 because an insufficient number of vessels were available for evaluation, and two subsequent evaluation time points indicated dramatic improvement in vessel shape measurements within this focal region. It is unknown whether this improvement in a focal area resulted from the effects of stroke or from the administration of bevacizumab.

For two other regions examined (Region 1 and the entire brain) bevacizumab therapy produced about a 20 point drop in MP, thus approaching the amount of improvement that we view as meaningful. Clinically, the patient appeared to respond to therapy. The overall MP nevertheless remained high (82 and 77 for Region 1 and the entire brain respectively), suggesting ongoing but perhaps reduced tumor activity. There was no obvious effect of bevacizumab upon the right frontal control region. Of importance, bevacizumab therapy did not, in and of itself, provide an immediate and dramatic normalization of vessel shape in sites in which vessels were clearly abnormal. Whether or not the efficacy of bevacizumab therapy can be assessed by measuring changes in vessel morphology on an individual basis is a topic for future research.

5.2 Limitations of the approach and comments on methodology

The major limitation of our approach is that it is not possible to evaluate vessels of diameter smaller than that of the voxel size used during image acquisition. For the $0.5 \times 0.5 \times 0.8$ mm³ voxels employed during our MRA acquisitions, the smallest visualizable vessels were 0.5mm in diameter (0.25mm radius). We therefore cannot visualize capillaries or tiny neoangiogenic sprouts. Other imaging methods, such as perfusion and permeability imaging, can provide different types of information about these smaller vessels, however. The two approaches appear to provide complementary information. Although perfusion/permeability imaging information was not available for this particular patient, it would be of high interest to perform a similar study incorporating both types of vessel analysis.

A second limitation of our approach is that we currently can define focal regions of interest only after a tumor has become visible by MR. However, once such a region has been identified, it appears that vessel shape abnormalities arise far earlier than the appearance of gadolinium enhancement. Global measurements performed over the entire brain can indicate that something is wrong but cannot provide information about where the problem lies. As previously noted, it would be helpful to develop a search program to define focal regions of vessel abnormality. We are currently working towards this goal using both search methods based upon vessel shapes themselves and search methods that use additional information provided by FLAIR images, perfusion and permeability imaging, diffusion imaging, and other imaging modalities.

The approach described in this report is potentially applicable to cancers arising at any location within the body. Abnormal vessel tortuosity is not unique to brain tumors, but instead appears to involve a wide range of common cancers including those of the breast (Lau et. al., 1999), colon (Siemann 2002), and lung (Helmlinger et. al., 2002). Extension of the method to anatomical regions outside of the brain requires methods of dealing with respiratory and cardiac motion, however. Such motion can blur small vessels during MRA acquisition, making them impossible to evaluate. Although computed tomographic angiography might provide a reasonable alternative to MRA, which takes a much longer time to acquire, traditional contrast agents may leak into the extravascular tissue, making it impossible to delineate vessels lying within the tumor confines. Further work is required before the approach can be readily extended to *in-vivo* imaging of anatomical regions subject to respiratory and cardiac motion.

5.3 Summary

This report analyzes vessel morphological changes as perceived by MRA of a single glioblastoma patient imaged over a four year period and during treatment by a variety of methods. Results suggest that vessel tortuosity abnormalities may resolve during successful therapy even with agents that are not specifically anti-angiogenic, that tumor resurgence is heralded by the development of focal vessel shape abnormalities months before any gadolinium enhancement is visible by MR, that total gross resection of an active focus is associated with an abrupt but transient drop in vessel shape abnormalities both focally and globally, and that anti-VEGF therapy does not necessarily induce rapid normalization of vessel shape. We believe that quantitative, statistical measures of vessel shape could provide an important tool both for the therapeutic monitoring of individual patients and for improving understanding of how cancers respond or fail to respond to various treatment modalities.

Acknowledgments

Funding Support

This work was supported by R01 EB000219 NIH-NIBIB and R01 CA124608 NIH-NCI. The funding source had no involvement in study design, data collection or analysis, the writing of the report, or in the decision to submit the paper for publication.

The paper is dedicated to an exemplary scientist and courageous patient who, knowing that he had been given the diagnosis of a malignant brain tumor, made the choice to pursue the current study, returning for repeated scans at his own initiative in the hope that something of value could be learned from his own experience.

Literature Cited

- Aylward SR, Bullitt E. Initialization, noise, singularities and scale in height ridge traversal for tubular object centerline extraction. *IEEE-TMI* 2002;21:61–75.
- Baish JS, Jain RK. Fractals and cancer. *Cancer Research* 2000;60:3683–3688. [PubMed: 10919633]
- Bullitt E, Gerig G, Pizer S, Aylward SR. Measuring tortuosity of the intracerebral vasculature from MRA images. *IEEE-TMI* 2003;22:1163–1171.
- Bullitt E, Ewend MG, Aylward S, Lin W, Gerig G, Joshi S, Jung I, Muller K, Smith JK. Abnormal vessel tortuosity as a marker of treatment response of malignant gliomas: Preliminary report. *Technology in Cancer Research and Treatment* 2004;3:577–584. [PubMed: 15560715]
- Bullitt E, Zeng D, Gerig G, Aylward SR, Joshi S, Smith JK, Lin W, Ewend MG. Vessel tortuosity and brain tumor malignancy: A blinded study. *Academic Radiology* 2005;12:1232–1240. [PubMed: 16179200]
- Bullitt E, Wolthuisen A, Brubaker L, Lin W, Zeng D, Van Dyke T. Malignancy-associated vessel tortuosity: A computer-assisted, MRA study of choroid plexus carcinoma in genetically engineered mice. *AJNR* 2006;27:612–619. [PubMed: 16552004]
- Bullitt E, Lin NU, Smith JK, Zeng D, Winer EP, Carey LA, Lin W, Ewend MG. Blood Vessel Morphological Changes as Visualized by MRA During Treatment of Brain Metastases. *Radiology* 2007;245:824–830. [PubMed: 17954616]
- Burger, PC.; Scheithauer, BW.; Vogel, FS. *Surgical Pathology of the Nervous System and its Coverings*. Vol. 3. Churchill Livingstone; New York: 1991.
- CBUTRUS: Central Brain Tumor Registry of the US. 2006. Available at <http://www.cbtrus.org/reports//2005-2006/2006report.pdf>
- Dempsey MF, Condon BR, Hadley DM. Measurement of tumor “size” in recurrent malignant glioma: 1D, 2D, or 3D? *AJNR* 2005;26:770–776. [PubMed: 15814919]
- Ferrara N, Carver-Moore K, Chen H, Dowd M, Lu L, Powell-Braxton L, Hillan KJ, Moore MW. Heterozygous embryonic lethality induced by targeted inactivation of the VEGF gene. *Nature* 1996;380:439–442. [PubMed: 8602242]
- Floeth F-W, Langen KJ, Reifenberger G, Weber F. Tumor-free survival of 7 years after gene therapy for recurrent glioblastoma. *Neurology* 2003;61:270–271. [PubMed: 12874421]
- Folkman J. Tumor angiogenesis: therapeutic implications. *New England Journal of Medicine* 1971;285:1182–1186. [PubMed: 4938153]
- Folkman J. Incipient Angiogenesis. *Journal of the National Cancer Institute* 2000;92:94–95. [PubMed: 10639502]
- Helmlinger G, Sckell A, Dellian M, Forbes NS, Jain RK. Acid production in glycolysis-impaired tumors provides new insights into tumor metabolism. *Clinical Cancer Research* 2002;8:1284–1291. [PubMed: 11948144]
- ICBM Atlas, McConnell Brain Imaging Centre. Montréal Neurological Institute, McGill University; Montréal, Canada:
- Iwadata Y, Fujimoto S, Namba H, Yamaura A. Promising survival for patients with glioblastoma multiforme treated with individualized chemotherapy based on *in vitro* drug sensitivity testing. *Brit. J. Cancer* 2003;89:1896–1900.
- Jain RK. Normalizing tumor vasculature with anti-angiogenic therapy: a new paradigm for combination therapy. *Nature Medicine* 2001;7:987–998.
- Krex D, Klink B, Hartmann C, von Deimling A, Pietsch T, Simon M, Sabel M, Steinbach JP, Heese O, Reifenberger G, Weller M, Schackert G. Long-term survival with glioblastoma multiforme. *Brain* 2007;130:2596–2606. [PubMed: 17785346]

- Lau DH, Xue L, Young LJ, Burke PA, Cheung AT. Paclitaxel (Taxol): an inhibitor of angiogenesis in a highly vascularized transgenic breast cancer. *Cancer Biother Radiopharm* 1999;14:31–6. [PubMed: 10850285]
- Li CY, Shan S, Huang Q, Braun RD, Lanzen J, Hu K, Lin P, Dewhirst MW. Initial stages of tumor cell-induced angiogenesis: evaluation via skin window chambers in rodent models. *J Natl Cancer Inst* 2000;92:143–147. [PubMed: 10639516]
- McDonald DM, Baluk P. Significance of blood vessel leakiness in cancer. *Cancer Research* 2002;62:5381–5385. [PubMed: 12235011]
- Parvez T. Glioblastoma multiforme treatment: Present trend in the primary treatment of aggressive malignant glioma: Glioblastoma multiforme. *Technology in Cancer Research and Treatment* 2008;7:241–248. [PubMed: 18473496]
- Price SJ, Jena R, Burnet NG, Hutchinson PJ, Dean AF, Pena A, Pickard JD, Carpenter TA, Gillard JH. Improved Delineation of Glioma Margins and Regions of Infiltration with the Use of Diffusion Tensor Imaging: An Image-Guided Biopsy Study. *AJNR* 2006;27:1969–74. [PubMed: 17032877]
- Reardon DA, Rich JN, Friedman HS, Bigner DD. Recent advances in the treatment of malignant astrocytoma. *JCO* 2006;24:1253–1265.
- Rueckert, D. Rview. 2002. Available: www.doc.ic.ac.uk/~dr/software
- Saaristo A, Veikkola T, Hytonen M, Arola J, Pajusola K, Turunen P, Jeltsch M, Karkkainen MJ, Kerjaschki D, Bueler H, Yla-Herttuala S, Alitalo K. Adenoviral VEGF-C overexpression induces blood vessel enlargement, tortuosity, and leakiness but no sprouting angiogenesis in the skin or mucous membranes. *The FASEB Journal* 2002;16:1041–1049. [PubMed: 12087065]
- Sampson JH, Archer GE, Bigner DD, Davis T, Friedman HS, Keler T, Mitchell DA, Reardon R, Sawaya R, Heimberger AB. Effect of EGFRvIII-targeted vaccine (CDX-110) on immune response and TTP when given with simultaneous standard and continuous temozolomide in patients with GBM. *J Clin Oncol* 2008 May 20;26(suppl)abstr 2011
- Schnabel JA, Rueckert D, Quist M, Blackall JM, Castellano Smith AD, Hartkens T, Penney GP, Hall WA, Liu H, Truwit CL, Gerritsen FA, Hill DLG, Hawkes JD. A generic framework for non-rigid registration based on non-uniform multi-level free-form deformations. *Lecture Notes in Computer Science* 2001;2208:573–581.
- Shukla D, Huilgol NG, Trivedi N, Mekala C. T2 weighted MRI in assessment of volume changes during radiotherapy of high grade gliomas. *J Cancer Res Ther* 2005;1:235–8. [PubMed: 17998661]
- Siemann D. Vascular Targeting Agents. *Horizons in Cancer Therapeutics* 2002;3:4–15.
- Stupp R, Dietrich P-Y, Kraljevic SO, Pica A, Maillard I, Maeder P, Meuli R, Janzer R, Pizzolato G, Miralbell R, Porchet F, Regli L, de Tribolet N, Mirimanoff I, Leyvraz S. Promising Survival for Patients With Newly Diagnosed Glioblastoma Multiforme Treated With Concomitant Radiation Plus Temozolomide Followed by Adjuvant Temozolomide 2002;20:1375–1382.
- Therasse P, Arbuck SG, Eisenhauer EA, et al. New guidelines to evaluate the response to treatment in solid tumors: European Organization for Research and Treatment of Cancer, National Cancer Institute of the United States, National Cancer Institute of Canada. *J Natl Cancer Inst* 2000;92:205–216. [PubMed: 10655437]
- Vredenburgh JJ, Desjardins A, Herndon JE, Marcello J, Reardon JA, Quinn JA, Rich JN, Sathornsumetee S, Gururangan S, Sampson J, Wagner M, Bailey L, Bigner DD, Friedman AH, Friedman HS. Bevacizumab plus Irinotecan in recurrent glioblastoma multiforme. *JCO* 2007;25:4722–4729.
- Warren KE, Patronas N, Aikin A, Albert PS, Balis FM. Comparison of One-, Two-, and Three-Dimensional Measurements of Childhood Brain Tumors. *JNCI* 2001;93:1401–1405. [PubMed: 11562391]
- Wildiers H, Guetens G, De Boeck G, Verbeken E, Landuyt B, Landuyt W, de Bruijn EA, van Oosterom AT. Effect of antivascular endothelial growth factor treatment on the intratumoral uptake of CPT-11. *J Pancreas* 2006;7:163–173.
- Willett CG, Boucher Y, Di Tomaso E, Duda DG, Munn LL, Tong RT, Chung DC, Sahani DV, Kalva SP, Kozin SV, Mino M, Cohen KS, Scadden DT, Hartford AC, Fischman AJ, Clark JW, Ryan DP, Zhu AX, Blaskowsky LS, Chen HX, Shellito PC, Lauwers GY, Jain RK. Direct evidence that the VEGF-specific antibody bevacizumab has antivascular effects in human rectal cancer. *Nat Med* 2004;10:145–7. [PubMed: 14745444]

- Wong ET, Brem S. Taming glioblastoma: targeting angiogenesis. *JCO* 2007;30:4705–4706.
- Wong MLH, Kaye AH, Hovens CM. Targeting malignant glioma survival signaling to improve clinical outcomes. *J Clin Neurosci* 2007;14:301–308. [PubMed: 17276069]
- Yoo MH, Hyun HJ, Koh JY, Yoon YH. Riluzole Inhibits VEGF-Induced Endothelial Cell Proliferation In Vitro and Hyperoxia-Induced Abnormal Vessel Formation In Vivo. *Investigative Ophthalmology and Visual Science* 2005;46:4780–4787. [PubMed: 16303979]
- Yuan F, Chen Y, Dellian M, Safabakhsh N, Ferrara N, Jain RK. Time-dependent vascular regression and permeability changes in established human tumor xenografts induced by an anti-vascular endothelial growth factor/vascular permeability factor antibody. *Proc Natl Acad Sci* 1996;93:14765–14770. [PubMed: 8962129]

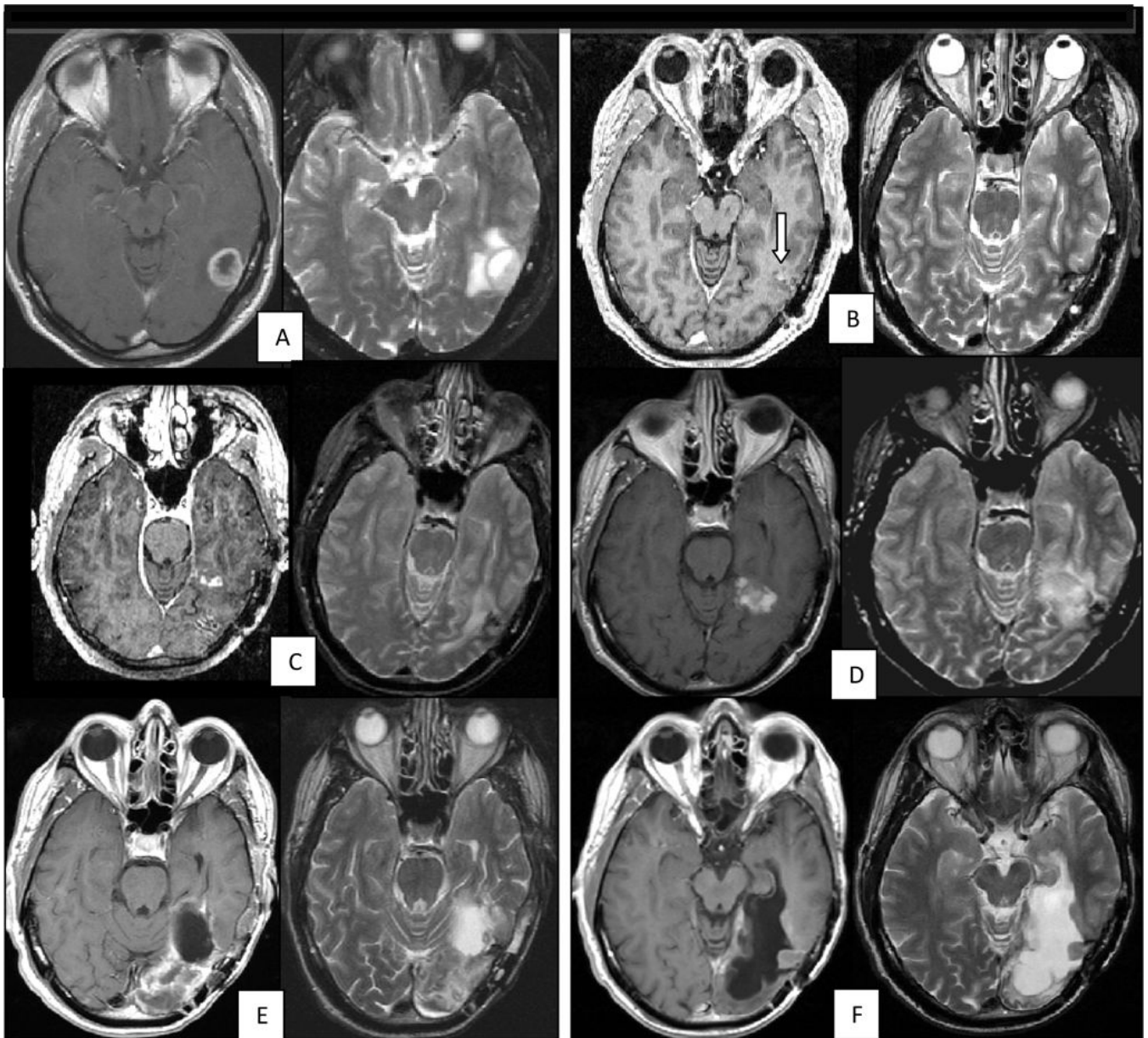


Figure 1.

T1-gadolinium enhanced (left) and T2 (right) MR slices obtained over time. A: Initial scan (month 0). Ring-enhancing tumor with a small amount of surrounding edema. B: Month 3. The tumor has been resected and radiation therapy delivered. There is no gadolinium enhancement and no edema. Arrow points to a gliadel wafer. C: Month 32. Development of a second lesion. D: Month 34. Enlargement of the second lesion and expansion of edema. E: Month 37. The second lesion has been resected. There is an emerging occipital lobe infarction. F: Month 48. Old occipital lobe infarction with patchy surrounding enhancement.

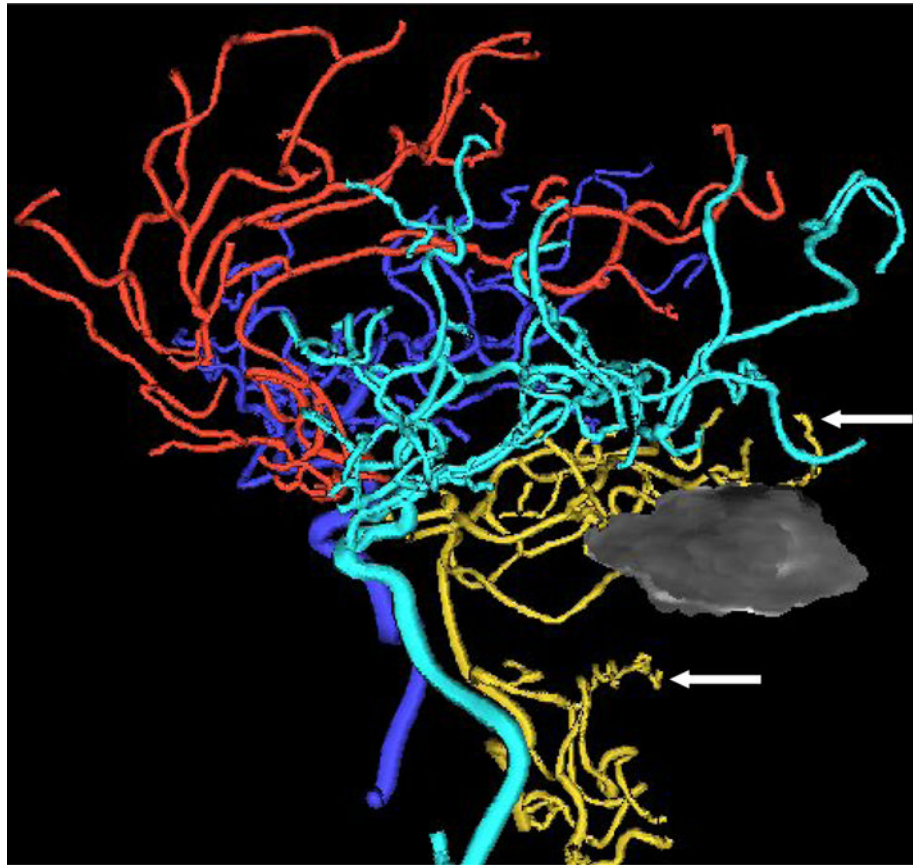


Figure 2. Vessels and segmented tumor/edema from Region 2. Red = anterior cerebral group, cyan = left middle cerebral group, blue = right middle cerebral group, gold = posterior cerebral group. Grey = tumor + edema as defined from T1 and registered into the coordinate system of the vessels. Arrows point to two vessels close to but outside of the apparent tumor confines and that exhibit abnormal, high-frequency, low-amplitude oscillations detectable by SOAM.

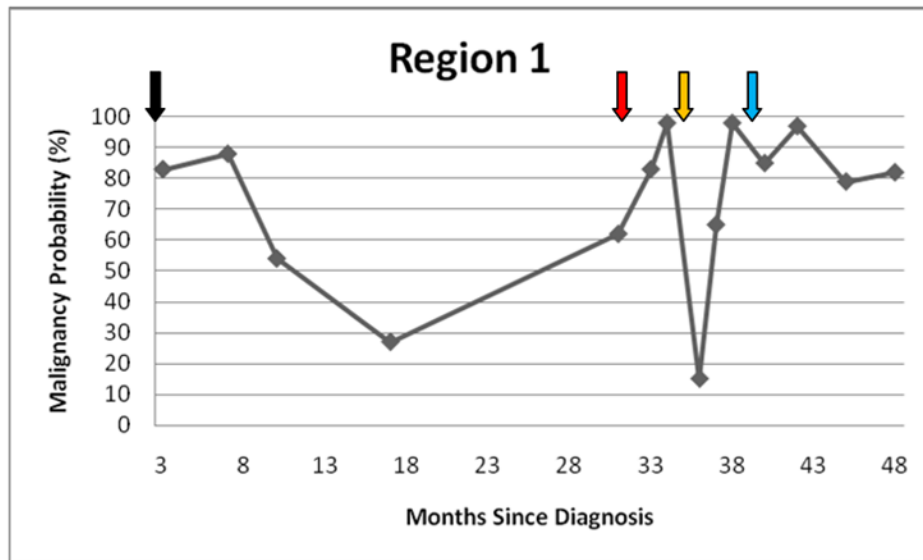


Figure 3. Malignancy Probability (MP) over time (months since diagnosis) in the region of the initial lesion. Black arrow: time of completion of radiation therapy. Red arrow: time at which a new gadolinium-enhancing lesion was first noted. Gold arrow: Total gross resection of new lesion. Blue arrow: initiation of bevacizumab therapy. An increase or decrease of 20 in the MP is viewed as significant.

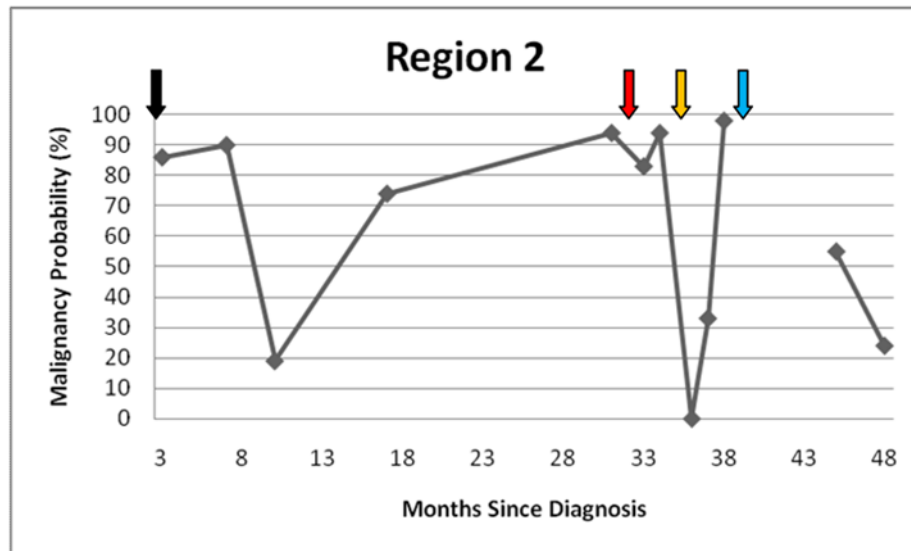


Figure 4. Malignancy Probability (MP) over time (months since diagnosis) in the region of the second lesion. Arrows provide the same time points as Figure 3. Two data points are missing because the patient suffered a stroke involving this region and an insufficient number of vessels were present for analysis.

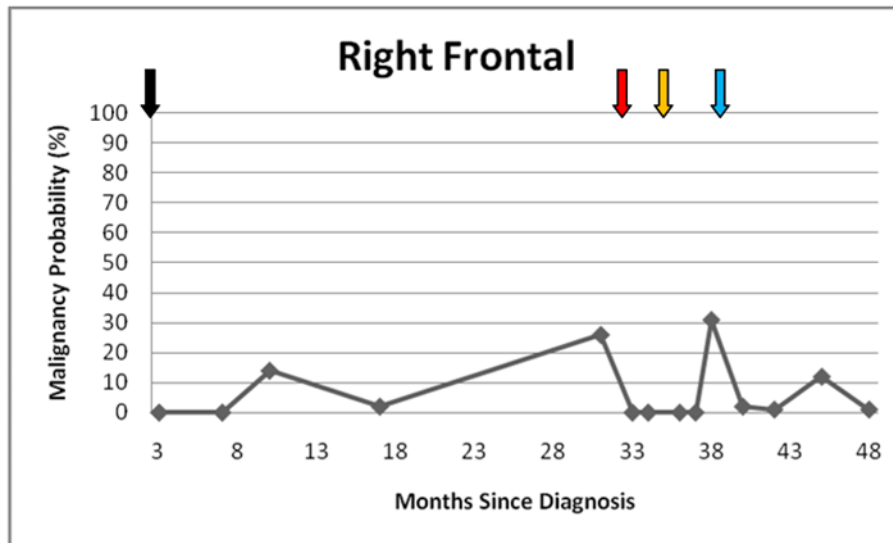


Figure 5. Malignancy Probability (MP) over time (months since diagnosis) in the control right frontal region. Arrows provide the same time points as Figure 3.

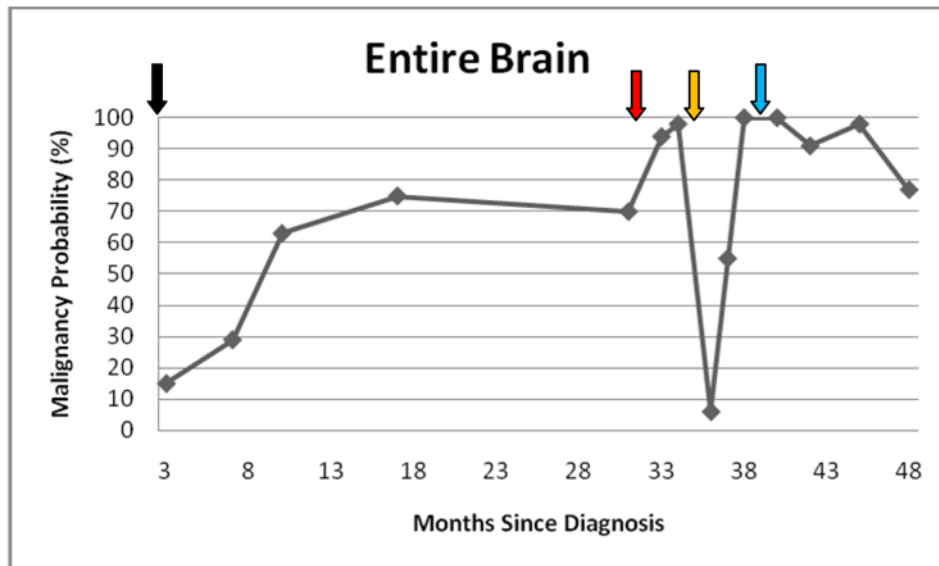


Figure 6. Malignancy Probability (MP) over time (months since diagnosis) in the entire brain. Arrows provide the same time points as Figure 3.

Table 1
Vessel attributes calculated over Region 1 (the initial lesion and surrounding edema).

| MONTH | nVC | nAVRAD | nSOAM | nICM | MP | Comment |
|-------|------|--------|-------|------|----|----------------------|
| 3 | 3.9 | -0.9 | 2.9 | -1.3 | 83 | RT completed month 3 |
| 7 | -1.0 | -1.5 | 2.4 | 0.0 | 88 | |
| 10 | 0.7 | -1.2 | 2.6 | -2.0 | 54 | |
| 17 | 0.9 | -0.9 | 1.4 | -1.0 | 27 | |
| 31 | -0.1 | -1.0 | 1.9 | -0.5 | 62 | |
| 33 | -0.1 | -0.7 | 2.4 | -0.4 | 83 | Lesion seen month 32 |
| 34 | 2.2 | -1.2 | 3.6 | -0.2 | 98 | |
| 36 | -0.3 | 3.4 | 0.8 | -0.6 | 15 | Resection month 35 |
| 37 | 1.7 | -0.8 | 2.2 | -0.9 | 65 | |
| 38 | 1.6 | -0.7 | 3.2 | 0.2 | 98 | Bevacizumab month 38 |
| 40 | -0.1 | -0.4 | 3.0 | -1.3 | 85 | |
| 42 | 0.9 | -1.1 | 3.3 | -0.2 | 97 | |
| 45 | -0.1 | -1.2 | 2.8 | -1.4 | 79 | |
| 48 | 0.7 | -1.2 | 2.6 | -0.8 | 82 | |

Month: month from the time of initial diagnosis. nVC: normalized (z-scored) vessel count. nAVRAD: z-scored average vessel radius. nSOAM: z-scored tortuosity as measured by the Sum of Angles Metric. nICM: z-scored tortuosity as measured by the Inflection Count Metric. MP: Malignancy Probability that represents a weighted combination of the nSOAM and nICM.

Table 2
Vessel attributes calculated over Region 2 (the second lesion and surrounding edema).

| MONTH | nVC | nAVRAD | nSOAM | nICM | MP | Comment |
|-------|------|------------------------------|-------|------|----|----------------------|
| 3 | 0.1 | -0.5 | 1.9 | 0.7 | 86 | RT completed month 3 |
| 7 | 0.1 | -1.0 | 2.5 | 0.0 | 90 | |
| 10 | 1.3 | -0.6 | 1.1 | -0.9 | 19 | |
| 17 | 2.9 | -0.1 | 2.3 | -0.5 | 74 | |
| 31 | 1.7 | -0.3 | 2.0 | 1.4 | 94 | |
| 33 | 0.5 | -0.4 | 2.2 | -0.1 | 83 | Lesion seen month 32 |
| 34 | 1.2 | 0.2 | 2.6 | 0.2 | 94 | |
| 36 | 0.1 | 4.5 | -0.2 | -1.6 | 0 | Resection month 35 |
| 37 | 0.1 | 0.1 | 0.6 | -1.1 | 33 | |
| 38 | 0.1 | 0.5 | 3.9 | -1.1 | 98 | Bevacizumab month 38 |
| 40 | | Too few vessels for analysis | | | | |
| 42 | | Too few vessels for analysis | | | | |
| 45 | -0.3 | -0.4 | 2.3 | -1.4 | 55 | |
| 48 | -0.3 | 0.1 | 1.4 | -1.0 | 24 | |

Month: month from the time of initial diagnosis. nVC: normalized (z-scored) vessel count. nAVRAD: z-scored average vessel radius. nSOAM: z-scored tortuosity as measured by the Sum of Angles Metric. nICM: z-scored tortuosity as measured by the Inflection Count Metric. MP: Malignancy Probability that represents a weighted combination of the nSOAM and nICM.

Table 3
Vessel attributes calculated over the right frontal (control) region.

| MONTH | nVC | nAVRAD | nSOAM | nICM | MP | Comment |
|-------|------|--------|-------|------|----|----------------------|
| 3 | -1.7 | 2.6 | -1.6 | -0.2 | 0 | RT completed month 3 |
| 7 | -0.9 | 0.5 | -1.1 | -1.6 | 0 | |
| 10 | -1.3 | 1.4 | 0.3 | 0.3 | 14 | |
| 17 | -0.1 | 1.4 | -0.3 | -0.4 | 2 | |
| 31 | -1.3 | 2.1 | 0.5 | 1.9 | 26 | |
| 33 | -1.7 | 1.8 | -1.7 | -1.6 | 0 | Lesion seen month 32 |
| 34 | -1.3 | 1.6 | -1.6 | -0.5 | 0 | |
| 36 | -1.7 | 6.0 | -1.3 | -0.8 | 0 | Resection month 35 |
| 37 | -0.9 | 2.9 | -1.7 | -1.5 | 0 | |
| 38 | -0.9 | 0.2 | 0.8 | 0.3 | 31 | Bevacizumab month 38 |
| 40 | -1.3 | 8.2 | -0.3 | -0.6 | 2 | |
| 42 | -1.3 | 1.5 | -0.6 | -0.6 | 1 | |
| 45 | -0.1 | 1.8 | 0.7 | -0.7 | 12 | |
| 48 | -0.9 | 3.1 | -1.0 | -0.7 | 1 | |

Month: month from the time of initial diagnosis. nVC: normalized (z-scored) vessel count. nAVRAD: z-scored average vessel radius. nSOAM: z-scored tortuosity as measured by the Sum of Angles Metric. nICM: z-scored tortuosity as measured by the Inflection Count Metric. MP: Malignancy Probability that represents a weighted combination of the nSOAM and nICM.

Table 4

Vessel attributes calculated over the entire brain.

| MONTH | nVC | nAVRAD | nSOAM | nICM | MP | Comment |
|-------|------|--------|-------|------|-----|----------------------|
| 3 | 0.4 | 0.4 | 1.7 | -2.1 | 15 | RT completed month 3 |
| 7 | -1.0 | -0.4 | 0.8 | 0.3 | 29 | |
| 10 | 0.5 | 0.3 | 2.8 | -2.0 | 63 | |
| 17 | -0.2 | 2.3 | 2.4 | -0.9 | 75 | |
| 31 | -0.2 | 1.9 | 2.6 | -1.5 | 70 | |
| 33 | 0.2 | 1.9 | 3.5 | -1.3 | 94 | Lesion seen month 32 |
| 34 | 0.2 | 1.9 | 4.0 | -1.0 | 98 | |
| 36 | -0.3 | 6.2 | 0.9 | -1.6 | 06 | Resection month 35 |
| 37 | 0.0 | 2.1 | 1.8 | -0.7 | 55 | |
| 38 | 0.9 | 1.6 | 5.8 | -1.6 | 100 | Bevacizumab month 38 |
| 40 | 0.1 | 2.5 | 4.5 | -0.5 | 100 | |
| 42 | -0.2 | 1.7 | 3.0 | -0.8 | 91 | |
| 45 | 0.3 | 1.9 | 4.6 | -2.1 | 98 | |
| 48 | 0.3 | 1.7 | 3.3 | -2.3 | 77 | |

Month: month from the time of initial diagnosis. nVC: normalized (z-scored) vessel count. nAVRAD: z-scored average vessel radius. nSOAM: z-scored tortuosity as measured by the Sum of Angles Metric. nICM: z-scored tortuosity as measured by the Inflection Count Metric. MP: Malignancy Probability that represents a weighted combination of the nSOAM and nICM.